New Phytologist

Research

Priority report

An emerging fungal disease is spreading across the globe and affecting the blueberry industry

Author for correspondence:
Michael Bradshaw
Email: mjbradsh@ncsu.edu

Received: *24 September 2024*
Accepted: *2 December 2024*

Michael Bradshaw[1,2], Kelly Ivors[3], Janet C. Broome[3], Ignazio Carbone[1], Uwe Braun[4], Shirley Yang[5], Emma Meng[5], Brooke Warres[3], William O. Cline[1], Swarnalatha Moparthi[1], Alejandro K. Llanos[6], Walter Apaza[6], Miao Liu[7], Julie Carey[7], Mehdi El Ghazouani[3], Rita Carvalho[3], Marianne Elliott[8], David Boufford[2], Tiaan Coetzee[3], Johan de Wet[3], James K. Mitchell[2], Luis Quijada[2,9], JamJan Meeboon[10], Susumu Takamatsu[11], Uma Crouch[1], Scott LaGreca[1] and Donald H. Pfister[2]

[1]Department of Entomology and Plant Pathology, Center for Integrated Fungal Research, North Carolina State University, Raleigh, NC 27606, USA; [2]Harvard University Herbaria and Department of Organismic and Evolutionary Biology, Harvard University, Cambridge, MA 02138, USA; [3]Global Plant Health, Driscoll's Inc., Watsonville, CA 95076, USA; [4]Department for Geobotany and Botanical Garden, Institute of Biology, Martin Luther University, Herbarium, Halle (Saale), 06108, Germany; [5]Department of Clean Stock, Driscoll's of China R&D, Yunshui Rd, DaBanQiao St., Central Yunnan New Industry Area, Kunming, 650000, Yunnan Province, China; [6]Department of Plant Pathology, Universidad Nacional Agraria La Molina, Ave La Molina s/n, La Molina, Lima, 15024, Peru; [7]Biodiversity and Bioresources, Ottawa Research and Development Center, Agriculture and Agri-Food Canada, 960 Carling Ave, Ottawa, ON, K1A 0C6, Canada; [8]Washington State University, Puyallup, WA 98371, USA; [9]Departamento de Botánica, Ecología y Fisiología Vegetal, Ave Astrofísico Francisco Sánchez, s/n. Facultad de Farmacia, Apartado 456, Código Postal 38200, San Cristóbal de La Laguna, Canary Islands, Spain; [10]Institute of Vegetable and Floriculture Science, National Agriculture and Food Research Organization (NARO), 360 Ano, Tsu, Mie, 514-2392, Japan; [11]Department of Bioresources, Graduate School, Mie University, 1577 Kurima-Machiya, Tsu, 514-8507, Japan

New Phytologist (2025)
doi: 10.1111/nph.20351

Key words: blueberries, co-evolution, emerging pathogens, fungi, powdery mildew.

Summary

- Powdery mildew is an economically important disease caused by *c*. 1000 different fungal species. *Erysiphe vaccinii* is an emerging powdery mildew species that is impacting the blueberry industry. Once confined to North America, *E. vaccinii* is now spreading rapidly across major blueberry-growing regions, including China, Morocco, Mexico, and the USA, threatening millions in losses.
- This study documents its recent global spread by analyzing both herbarium specimens, some over 150-yr-old, and fresh samples collected world-wide.
- Our findings were integrated into a 'living phylogeny' via T-BAS to simplify pathogen identification and enable rapid responses to new outbreaks. We identified 50 haplotypes, two primary introductions world-wide, and revealed a shift from a generalist to a specialist pathogen.
- This research provides insights into the complexities of host specialization and highlights the need to address this emerging global threat to blueberry production.

Introduction

Understanding the dynamics and spread of plant pathogens is critical for the development of effective management strategies. Powdery mildews, a group of obligate parasitic fungi, exemplify this challenge, having a profound impact on a multitude of plant species, including economically significant crops and ornamentals such as wheat, grapes, blueberries, hops, peas, and strawberries. Recent advances in genetic research have shed light on the host specificity of these pathogens, suggesting a much more complex

interaction with their hosts than previously understood (Vaghefi *et al.*, 2022; Bradshaw *et al.*, 2022a, 2024a,b; Kusch *et al.*, 2024). A comprehensive understanding of the taxonomy and evolutionary relationships of powdery mildews is essential, given their invasive behavior and potential to cause significant ecological and agricultural damage (Johnson *et al.*, 1979; Bebber *et al.*, 2014; Fuller *et al.*, 2014; Kiss *et al.*, 2020; Bradshaw *et al.*, 2021).

Originating in Eastern North America, *Erysiphe vaccinii* Schwein. is a powdery mildew fungus that primarily infects the Ericaceae, showing a strong affinity for species of *Vaccinium*, notably blueberries (Braun & Cook, 2012). This pathogen poses a considerable risk to the blueberry industry by reducing crop yields and increasing reliance on fungicides. A noteworthy aspect of *E. vaccinii*, which was previously classified under the names '*Erysiphe vaccinii*' and '*Erysiphe elevata*', includes its infection of diverse hosts such as cultivated blueberries (*Vaccinium corymbosum*), *Catalpa* spp. (Bignoniaceae), and *Eucalyptus* spp. (Myrtaceae). Single-locus rDNA phylogeny previously grouped these pathogens into a highly supported clade named 'the *Erysiphe vaccinii* complex' (Tymon *et al.*, 2022), highlighting their close genetic relationship and identical morphology despite infecting unrelated host species.

Dramatic growth in global production and trade of blueberries has been driven by mounting consumer demand and as blueberry production has expanded across the globe, so has its pests. In this study, we have detected *E. vaccinii* in blueberry-growing regions world-wide, marking its first reported occurrence outside North America (Bradshaw *et al.*, 2024a) and signifying its status as an emergent pathogen. We uniquely combined a global collection of *E. vaccinii* from blueberry farms and herbarium specimens, some dating back over 150 yr. We sequenced six genetic loci from these specimens to shed light on the phylogeny, taxonomy, and population structure of this emerging threat. Our goals were to explore the diversity of the pathogen, its range of hosts, and the evolutionary dynamics of its spread over time and space. By integrating our findings into a 'living phylogeny' through an online phylogeny database (T-BAS), we aimed to simplify pathogen identification for both specialists and nonexperts, facilitating rapid response to outbreaks. Through this approach, we sought to better understand the spread of *E. vaccinii* and provide valuable information to the expanding blueberry industry to help better understand this pathogen and its world-wide impacts.

Materials and Methods

Morphological examinations

Morphological examinations were accomplished following Bradshaw *et al.* (2022b). Morphological examinations of the asexual morph of recently collected samples were accomplished by placing clear adhesive tape on powdery mildew colonies and setting the tape onto a slide containing a drop of water, or by doing hand sections and mounting them onto a slide with potassium hydroxide (KOH), Melzer's reagent (MLZ), or Congo red. Examinations of the sexual morph were accomplished by using a clean needle to mount chasmothecia onto a microscope slide containing water, KOH, MLZ, or Congo red. Photographs were taken of the slides using a compound microscope with an Olympus SC50 camera (Tokyo, Japan) and a Zeiss AX10 microscope.

Sequencing

DNA extractions were accomplished using the Chelex method (Walsh *et al.*, 1991; Hirata & Takamatsu, 1996). The Polymerase chain reaction (PCR) was carried out for the Internal Transcribed Spacer rDNA (ITS) and Large Subunit rDNA (LSU) region using the primer pairs PM10/PM28R (Bradshaw & Tobin, 2020). If PCR was unsuccessful, a nested approach was applied using the primers AITS (Bradshaw & Tobin, 2020)/TW14 (Mori *et al.*, 2000) followed by PM10/PM28R or AITS/PM11 (Bradshaw & Tobin, 2020) followed by PM10/PM2 (Cunnington *et al.*, 2003). For the *CAM*, *GAPDH*, *GS*, and *RPB2* region the primer pairs PMCAM1/PMCAM4R, PMGAPDH1/PMGAPDH3R, GSPM2/GSPM3R, and PMRpb2_4/PMRpb2_6R were used (Bradshaw *et al.*, 2022a). If these were unsuccessful for the *GS* and *RPB2* regions, the following primers from Bradshaw *et al.* (2023) were used: EGS1/EGS2R and ERPB2_3/ERPB2_7R. For the TUB region the primers BTF5b/BTR7a (Ellingham *et al.*, 2019) were used followed by ETUB2 and ETUB2R (Bradshaw *et al.*, 2023). Often the *GAPDH* sequences were contaminated with *Ampelomyces* and as such the primers EGAPDH1/EGAPDH2 (Bradshaw *et al.*, 2024b) were used if sequencing failed from PMGAPDH1/PMGAPDH3R.

Reference phylogenetic trees

A representative tree of taxa with a complete 7 loci dataset (except *E. vaccinii* f. *eucalyptorum*) from the *E. vaccinii* complex was generated from the concatenated ITS + LSU + *CAM* + *GAPDH* + *GS* + *RPB2* + TUB sequences. In addition, single-locus trees were constructed from all the newly generated sequences. Sequences were aligned and edited using MUSCLE in MEGA11 (Tamura *et al.*, 2021). A GTR + G + I evolutionary model was used for phylogenetic analyses as it is the most inclusive model of evolution and includes all other evolutionary models (Abadi *et al.*, 2019). The phylogeny was inferred using Bayesian analysis of the combined loci using a Yule tree prior (Gernhard, 2008) and a strict molecular clock, in the program BEAST v.1.10.4 (Suchard *et al.*, 2018). A single MCMC chain of 10^7 steps was run, with a burn-in of 10%. Posterior probabilities were calculated from the remaining 9000 sampled trees. A maximum clade credibility tree was produced using TREEANNOTATOR v.1.10.4 (part of the BEAST package). Stationarity was confirmed by running the analysis multiple times, which revealed convergence between runs. The resulting tree was visualized using FIGTREE v.1.3.1 (Rambaut, 2009). A maximum likelihood analysis was accomplished using RAXMLGUI (Silvestro & Michalak, 2012) under the default settings with a GTR + G + I evolutionary model. Bootstrap analyses were conducted using 1000 replications (Felsenstein, 1985).

A separate multilocus phylogeny was inferred for a total of 50 *Erysiphe* strains that were genotyped across seven loci (*CAM*, *GAPDH*, *GS*, ITS, LSU, *RPB2*, *TUB*). Multiple sequence alignments were generated for each locus using MAFFT, concatenated, and subjected to maximum likelihood phylogenetic

inference using RAxML; support values for each node in the tree were calculated using 1000 bootstrap replicates. The concatenated maximum likelihood approach was compared to the Bayesian approach implemented in BEAST v.1.10.4 and to a multispecies coalescent model implemented in ASTRAL-III v.5.7.8 (Zhang *et al.*, 2018). The best tree, alignments, and specimen metadata (e.g. host, locality) were uploaded to T-BAS (Carbone *et al.*, 2017, 2019) to enable real-time phylogeny-based placement of unknown *Erysiphe* strains for any number of the seven loci in the reference tree. The reference tree is available for viewing and placement on the T-BAS guide page (https://guide-tbas.cifr.ncsu.edu/tbas).

Phylogeny-based placement

Multilocus sequence data for a total of 123 strains of *E. vaccinii* isolated from different hosts were phylogenetically placed into the *Erysiphe* reference tree using T-BAS and the EPA-NG v.0.3.8 algorithm (Barbera *et al.*, 2019) implemented at CIPRES (Miller *et al.*, 2015). In T-BAS, the placements are visualized and standardized using a Metadata Enhanced PhyloXML (MEP) format. This standardization allows placements and associated specimen attributes (e.g. host, locality) to be readily viewed, archived, and importantly analyzed within a phylogenetic context. For example, sequences can be filtered for a user-specified number of loci, and the corresponding multiple sequence alignments, associated metadata, and Newick tree can be downloaded for downstream analyses.

Population structure

Genetic admixture among formae was examined using STRUCTURE v.2.3.4 (Pritchard *et al.*, 2000; Falush *et al.*, 2003) and by using computational resources accessible via the CIPRES REST API (Miller *et al.*, 2015). To reduce the potential for nonrandom missing data bias (Yi & Latch, 2022), the analysis was based only on 136 out of 173 strains with available sequence data for at least five of the seven reference loci (*CAM*, *GAPDH*, *GS*, ITS, LSU, *RPB2, TUB*). For each *Erysiphe* forma, estimators of population mean mutation rate (θ) and pairwise nucleotide diversity (π) were calculated using the program SITES v.1.1 (Hey *et al.*, 2018). Neutrality tests were performed to test for population size constancy using Tajima's *D* (Tajima, 1989), Fu and Li's *D* and Fu and Li's *D** (Fu & Li, 1993), also implemented in SITES. Individuals were assigned to $k = 10$ possible clusters using PARALLELSTRUCTURE (Besnier & Glover, 2013) with three independent replicates for each *k* value. Membership probabilities were based on a MCMC burn-in of 50 000 steps followed by 100 000 sampling iterations. Optimal *k* values were examined using $\log_e P(D)$ and delta *K* methods (Evanno *et al.*, 2005) implemented in STRUCTURE HARVESTER v.0.6.93 (Earl & vonHoldt, 2011). Cluster membership results were visualized using histograms in outer rings of the phylogeny with placements results using the structure tool in DECIFR (https://tools.cifr.ncsu.edu/structure).

Network and haplotype inference

Network inference was based on parsimony and neighbor-joining methods implemented in TCS1.21 (Clement *et al.*, 2000) and SPLITSTREE4 v.4.14.8 (Huson, 1998), respectively. In TCS, sequences were collapsed into haplotypes with gaps treated as missing data. Nodes were colored as a function of host and geographical location, and node size was proportional to haplotype frequency. The Neighbor-net algorithm implemented in SPLITSTREE was used to further identify splits or bipartitions in the data, where the presence of multiple parallel edges between bipartitions indicates a history of recombination; in the absence of phylogenetic conflict, splits would be separated by a single edge. Recombination among formae was further tested using the pairwise homoplasy index (PHI) implemented in SPLITSTREE.

Multilocus isolation with migration

For each locus, a single recombination-free partition was extracted from the multiple sequence alignment using the four-gamete criterion to identify the largest interval of compatible single nucleotide polymorphisms, as implemented in the IMgc program (Woerner *et al.*, 2007). The best time-ordered rooted topology of formae was determined by performing topology sampling runs with hyperpriors under an infinite-sites mutation model using IMA3 v.1.11 (Hey & Wakeley, 1997). Population parameter estimates of migration rates ($2N_em$), splitting times (t), and effective population size (N_e) were performed using the fixed best-rooted topology. Markov chain Monte Carlo (MCMC) runs were based on a burn-in of 1000 000 steps, 256 heated chains using a geometric heating scheme of parameters ha = 0.97 and hb = 0.8, 10 000 sampled genealogies, a mutation rate 1×10^{-9} per base per generation, and a generation time of 1 yr due to the chasmothecia needing to perennate for ascospore discharge and germination (Salmon, 1900; Homma, 1937; Jailloux *et al.*, 1998; Jarvis *et al.*, 2002; Braun & Cook, 2012). Mutation rates can span several orders of magnitude ranging from 4.5×10^{-7} mutations per base pair per generation in *Blumeria graminis* f. sp. *tritici* (Sotiropoulos *et al.*, 2022) to 2.0×10^{-8} in *Schizophyllum commune* (Baranova *et al.*, 2015) and as low as 4.2×10^{-11} in *Aspergillus flavus* (Álvarez-Escribano *et al.*, 2019). Because there are no reported estimates of mutation rates in *Erysiphe* we assumed a conservative estimate of 1×10^{-9} per base per generation that is typical of many fungi (Edwards & Rhodes, 2021). In IMA3 simulations convergence in parameter estimates was based on two runs each with swapping rates > 0.9 and effective sample sizes in excess of 10 000. The best-rooted phylogeny was redrawn to include population parameter estimates and visualized using the IMFIG program (https://github.com/jodyhey/IMa3). All runs were performed using tools in DECIFR, working seamlessly with computational resources at CIPRES.

Results

Sample collection

During a comprehensive global survey of fresh material and herbarium specimens spanning Canada, China, Mexico, Morocco, South Africa, Peru, Portugal, and the USA, we have successfully sequenced 173 specimens of powdery mildew, all part of the *E. vaccinii* complex. These specimens were gathered from a wide

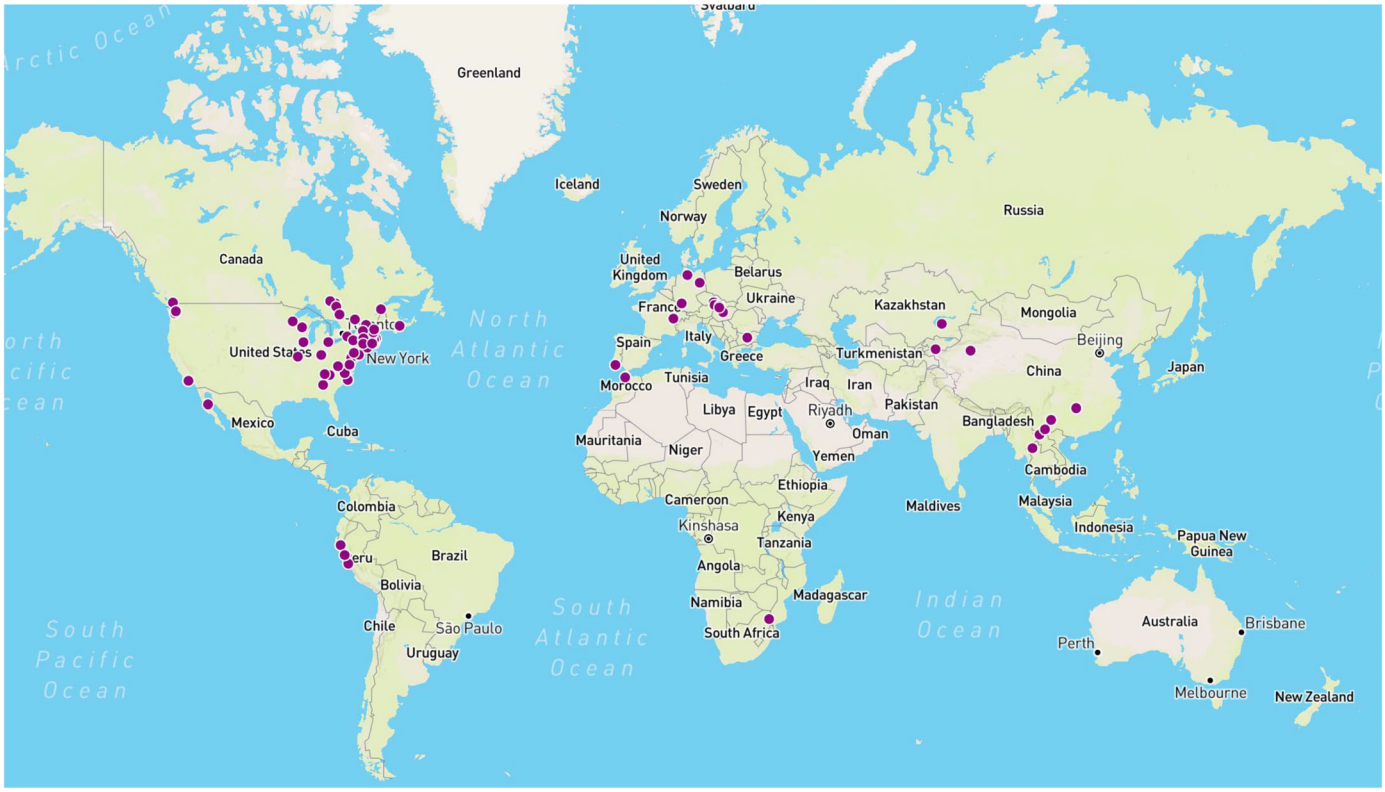

Fig. 1 World map of the specimens collected for the present study generated using Mapbox (https://www.mapbox.com/) implemented in T-BAS.

array of host species including *Catalpa bignoniodes*, *Catalpa speciosa*, *Epigaea repens*, *Eucalyptus camaldulensis*, *Gaultheria shallon*, *Gaylussacia baccata*, *Gaylussacia frondosa*, *Kalmia latifolia*, various *Vaccinium* hybrids from the North Carolina State University (NCSU) blueberry breeding program, *V. corymbosum*, *Vaccinium macrocarpon*, *Vaccinium myrtilloides*, *Vaccinium myrtillus*, *Vaccinium pallidum*, *Vaccinium parvifolium*, and *Vaccinium virgatum* (Fig. 1; Supporting Information Table S1).

Economic cost of powdery mildew to the blueberry industry

The growers and Global Plant Health research colleagues participating in the study indicate that powdery mildew on blueberries was first identified on blueberry outside North America in Portugal in 2012, followed by detections in Honghe, China (2016), Hoedspruit, South Africa (2018), Viru, Peru (2019), Olmos, Peru, and Banna, China (2020), Baja, Mexico and Qujing, China (2021), and Barranca, Peru (2022) (Table S2). Although we reached out to growers and extension agents in Washington and Oregon, states where blueberries are widely cultivated and conditions are highly favorable for powdery mildew, no instances of infected blueberries were reported.

As of 2021 the global highbush blueberry planting area had reached 235 408 ha (Zang, 2022). Growers estimated the cost of powdery mildew control to range from $200 to $2250 per hectare (Table S2). As such, these figures suggest that powdery mildew could impose an annual cost of $47 to $530 million to the blueberry industry globally.

Morphology

Our analysis of powdery mildew specimens from outside eastern North America revealed a dominant asexual reproductive stage, marked by extensive conidiophore production (Fig. 2), throughout the growing season. Moreover, no sexual stage was observed on any blueberry specimens from these regions. This uniform presence of the asexual state suggests that a single mating type has been introduced globally from eastern North America. Notably, samples of *E. vaccinii* f. *convertibilis* displayed only asexual stages. Interestingly, North American samples within this clade were exclusively identified in greenhouse settings that were part of the NCSU blueberry breeding program. Analysis showed *E. vaccinii* f. *vaccinii-corymbosi* split into two subclades (Figs 3, 4, S2). One included all specimens from outside North America as well as a greenhouse specimen from the NCSU breeding program, all of which exhibited only the asexual state. This indicates that all of the strains proliferating globally and requiring significant management efforts (Table S2) propagate exclusively through asexual means. However, powdery mildew infecting blueberry farms in North Carolina exhibit only mild symptoms in midsummer followed by a prominent sexual reproductive phase that occurs late in the season. Although those farms report a high incidence of the disease (Table S2), there is only a minimal effect on crop yield. We hypothesize that the negligible impact on crop yield observed in North Carolina is likely attributed to environmental factors, and growing conditions (in California, China, Mexico, Portugal and Morocco blueberries tend to be grown

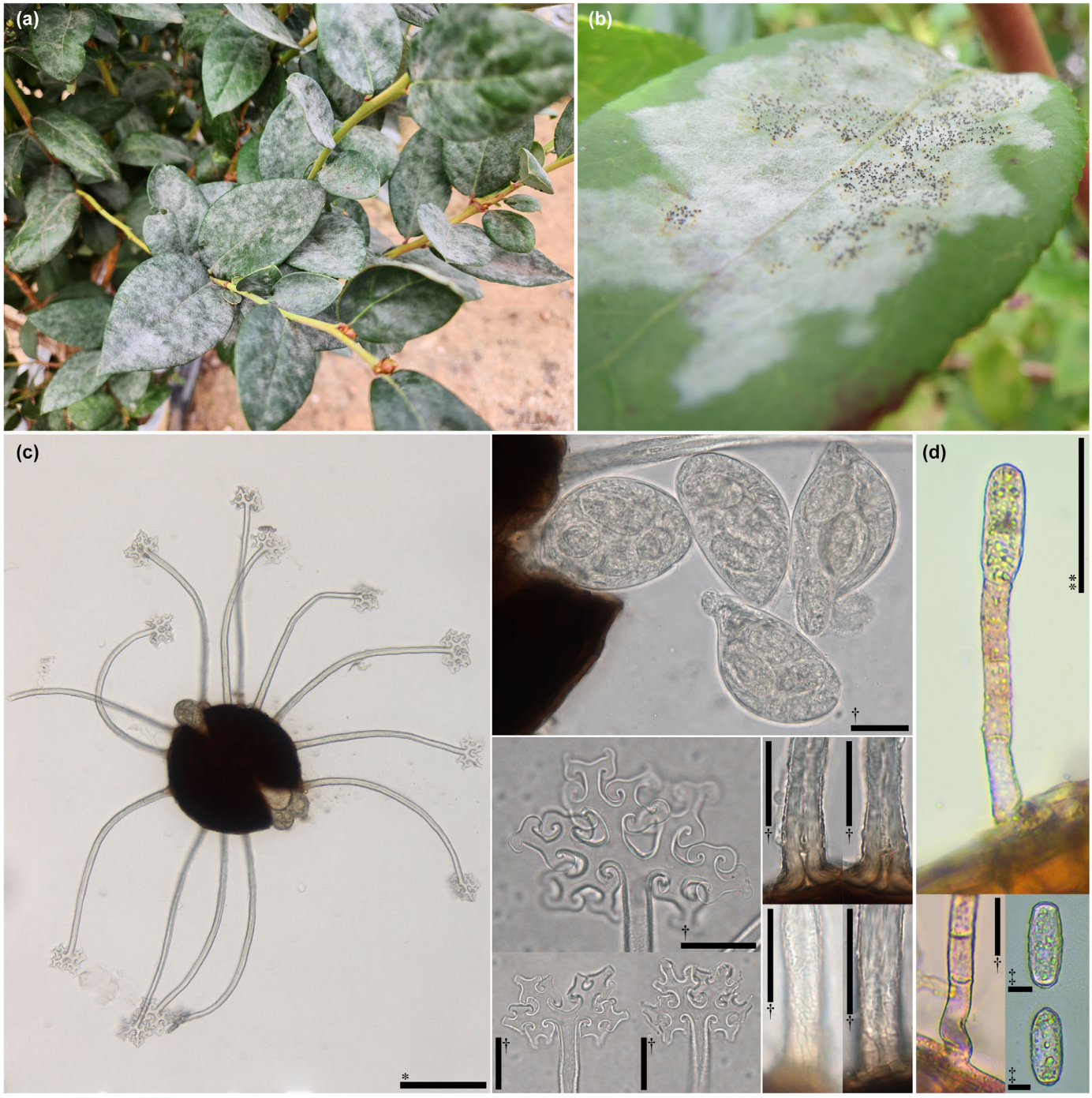

Fig. 2 Powdery mildew infecting blueberries. (a, b) Powdery mildew infecting leaves. (c) Sexual (overwintering) stage from eastern North America, consisting of chasmothecia, asci and ascospores. (d) Asexual stage, from California, consisting of conidiophores, and conidia. Bars: (*) 100 μm; (**) 50 μm; (†) 20 μm; (‡) 10 μm.

in hoop houses). It could also stem from the fungus manifesting earlier in the season with heightened virulence due to it only forming an asexual phase.

Phylogeny and population genetics

The multilocus reference phylogeny of *Erysiphe* is shown in Fig. 3. There was no significant difference in the topology of the tree inferred from three commonly used phylogenetic inference methods (Fig. S1). Phylogenetic, network, and multilocus isolation with migration analyses (Figs 3, 4, S1, S2) confirm the distinctiveness and host specificity of *E. vaccinii*, which led to our classification of this species into different formae based predominantly on host range (Bradshaw *et al.*, 2024b). In the current study three different formae infecting blueberries have been identified, although

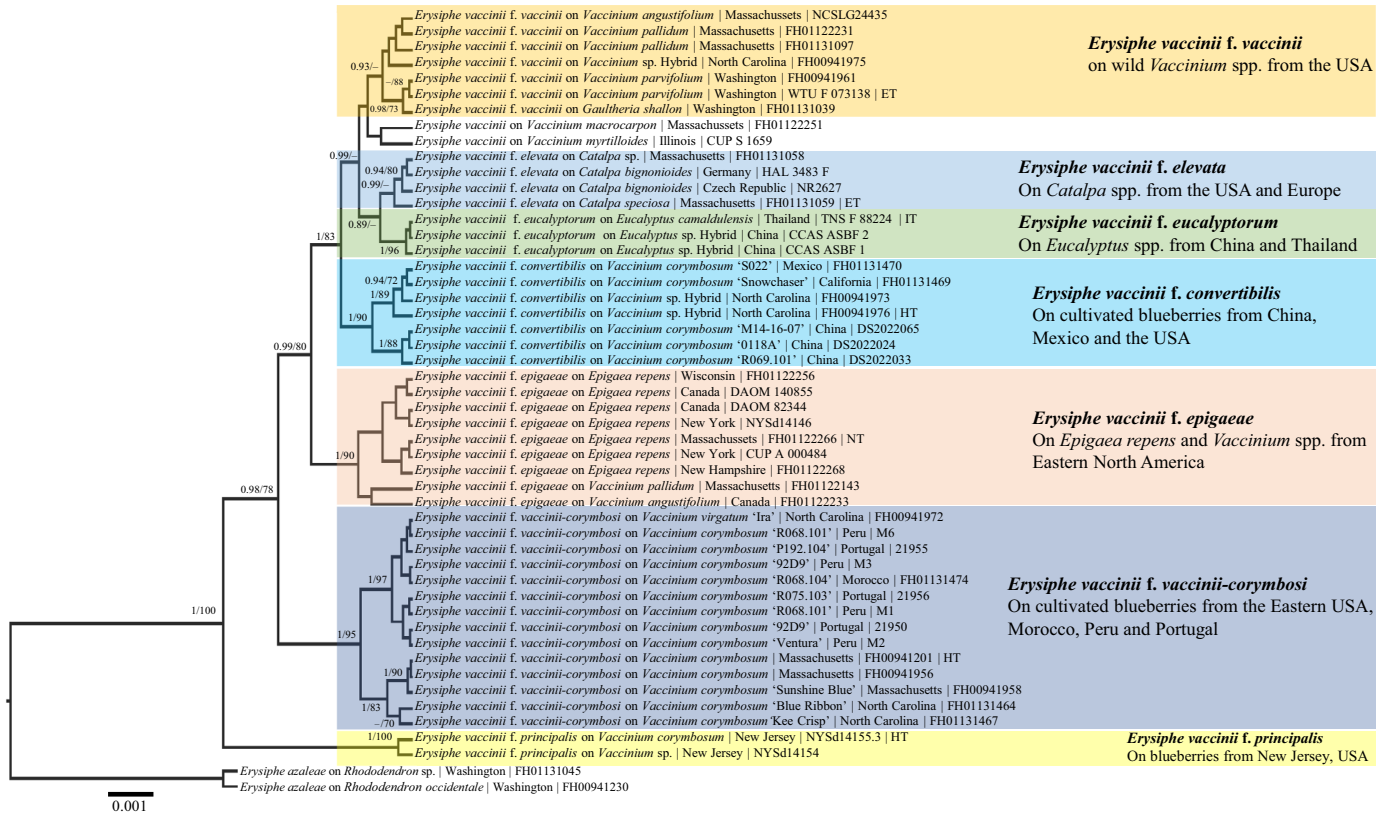

Fig. 3 Bayesian maximum clade credibility tree of the concatenated ITS + LSU + *CAM* + *GAPDH* + *GS* + *RPB2* + TUB regions of select taxa in the '*Erysiphe vaccinii* complex' with complete genetic data (except for *E. vaccinii* f. *eucalyptorum*). The phylogenetic tree revealed two different formae that are spreading throughout the world infecting blueberries. The fungal formae are denoted followed by the host, collection locality, and voucher number. Type status (HT, IT, ET, NT) of the specimens concerned is denoted. Posterior probabilities ≥ 90 are displayed followed by bootstrap values > 70% for the maximum likelihood (ML) analyses conducted.

E. vaccinii f. *principalis*, was found only on specimens over 100-yr-old, and thus seems irrelevant to current blueberry cultivation.

Our analyses revealed 50 multilocus haplotypes, with a notable bottleneck effect in China (H0), Morocco (H42, H44), Portugal (H42), and Peru (H42, H43), indicated by a single or shared

Fig. 4 Phylogenetic and population structure inference. (a) The best maximum likelihood tree obtained from a multilocus phylogeny-based placement of 123 strains on the *Erysiphe vaccinii* reference tree. The numbers along the edges are node support values in the reference tree based on 1000 bootstrap replicates. Only strains with sequences for at least five of the seven reference loci (*CAM*, *GAPDH*, *GS*, ITS, LSU, *RPB2*, *TUB*) were retained for population genetic analysis and shown on the tree. Colorized rings around the tree are used to show different strain attributes. The inner ring displays 50 multilocus haplotypes followed by a ring for the different *E. vaccinii* formae. The two outer rings display optimal STRUCTURE admixture results of $k = 2$ and $k = 7$, based on delta K and $\log_e P(D)$ methods, respectively; the corresponding plots of delta K and $\log_e P(D)$ values with predefined $k = 1$–10 are shown below the tree with error bars showing SD per cluster (K). Two genetically distinct clusters delineate the two outgroups: *Erysiphe azaleae* and *E. vaccinii* f. *principalis*. (b) Statistical parsimony haplotype networks. Two networks were inferred for the 50 multilocus haplotypes using a 95% parsimony connection limit: one large reticulating network and a smaller satellite network including the two strains from *Rhododendron*. The nodes in the network are replaced with pie diagrams depicting the frequency of haplotype sharing by different hosts. Six haplotypes occupy interior positions in the network and include strains from different hosts; 15 tip haplotypes are singletons and host specific. The *E. vaccinii* samples from *Vaccinium corymbosum* belong to least two distinct clonal lineages with evidence of recent clonal expansion. (c) SPLITSTREE haplotype network. A splits graph generated for the in group *E. vaccinii* strains showing five distinct bipartitions or splits in the data. The *E. vaccinii* that are not assigned to a host belong to two different bipartitions. The presence of multiple parallel edges between the five bipartitions indicates a history of recombination within formae but very limited recombination between formae on a modern time scale; in the absence of phylogenetic conflict, splits would be separated by a single edge. The bar is proportional to the weight of the split computed using the Neighbor-net algorithm. (d) Multilocus isolation with migration analysis for *E. vaccinii* formae. The phylogeny with the highest estimated posterior probability is represented as a hierarchical series of boxes with interior ancestor boxes connecting descendant populations where the width of boxes is proportional to the estimated N_e. The 95% confidence intervals for each N_e value are shown as dashed lines to the right of the left side of the corresponding population box. Gray arrows to the 95% N_e intervals extend on either side of the right side of each population box. Splitting times, positioned at even intervals, are depicted as solid horizontal lines, with text values on the left in units of thousand years ago. In the phylogeny *E. vaccinii* f. *vaccinii* and *E. vaccinii* f. *vaccinii-corymbosi* are recently evolved populations and there is no evidence of significant gene flow among formae. Divergence time estimates assumed a generation time of 1 yr and a mutation rate of 1×10^{-9} per base per generation.

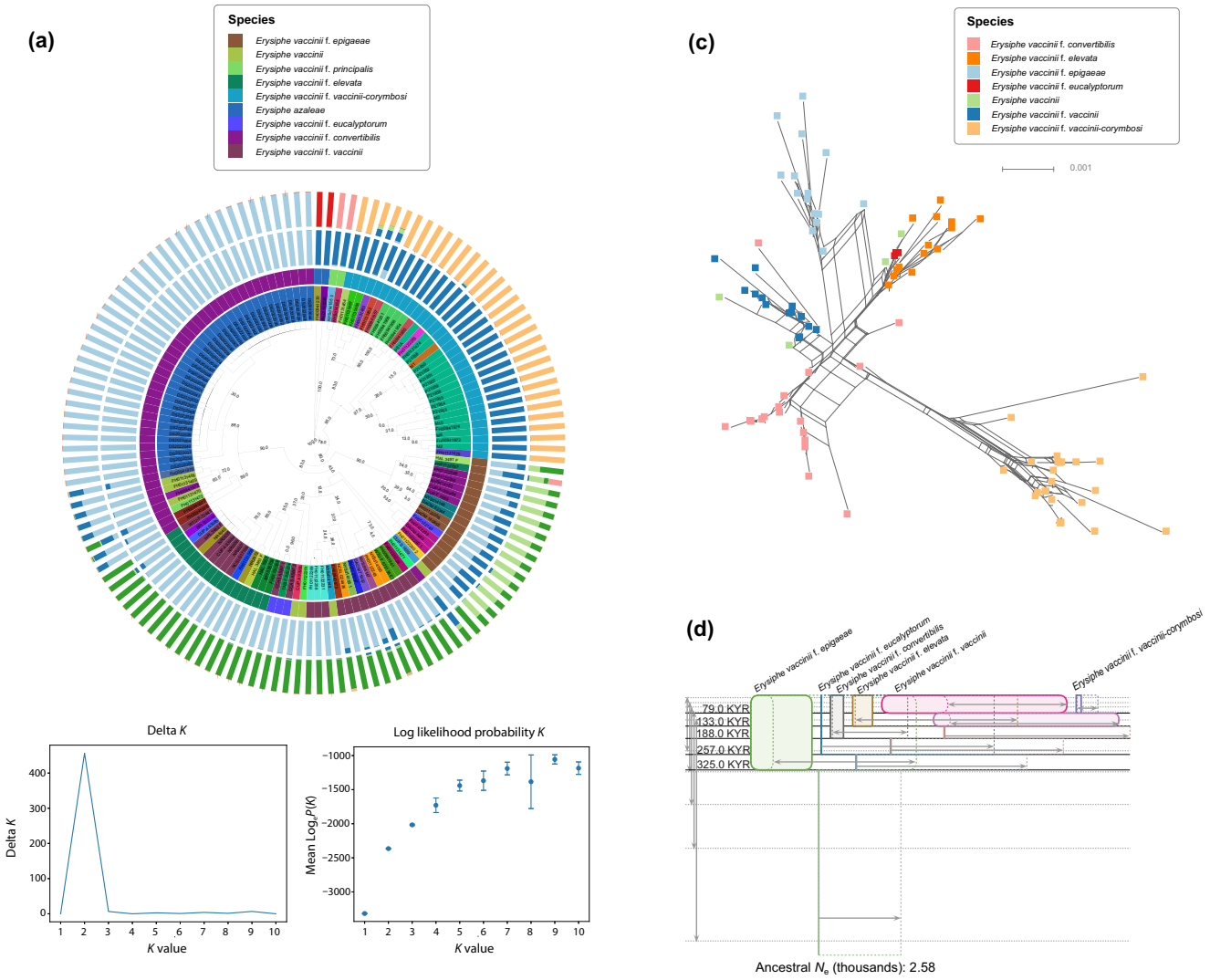

haplotype in each geographic region despite extensive sampling (Table S3; Fig. S2). The data indicate two primary introductions of *E. vaccinii* – *E. vaccinii* f. *convertibilis* to China, Mexico, and California, and *E. vaccinii* f. *vaccinii-corymbosi* to Morocco, Peru, and Portugal (Figs 3, 4a, S3). This is further supported by significant negative values for Fu and Li's *D* and Fu and Li's *D** for variation in TUB and *CAM*, indicative of population expansion (Table S4). Minimal genetic diversity was observed outside Eastern North America compared to high diversity within North America, suggesting origin of the pathogen in this region, which is consistent with the native range of its blueberry host.

The haplotype network based on host (Fig. 4b) indicates that the powdery mildews studied evolved from generalist to specialist in support of the specialization hypothesis (Futuyma & Moreno, 1988). Additionally, the SplitsTree graph (Fig. 4c) showed significant evidence of recombination within formae ($P < 0.005$) but limited recombination between formae. All formae, with the exception of *E. vaccinii* f. *convertibilis*, are represented by specimens dating back to the 1800s. Tests of isolation with migration did not detect any significant gene flow among formae (Fig. 4d). Gene flow among the different formae, if it exists, is both limited and ancient. The smallest effective population size estimates were for *E. vaccinii* f. *vaccinii-corymbosi* (5160–19 350 individuals) and *E. vaccinii* f. *convertibilis* (10 320–63 210). Overall divergence time estimates ranged from 79 to 325 thousand years ago (ka) indicating that formae evolved on an evolutionary time scale and before the development of agriculture (*c.* 12 ka). This underscores their ancient origins, suggesting they are not the result of recent evolutionary changes or modern agricultural practices.

Discussion

This study provides a comprehensive look into the evolution and spread of powdery mildews on blueberries, emphasizing its significant impact on the global blueberry industry. By leveraging a 'living phylogeny' through T-BAS (Carbone *et al.*, 2019) and examining herbarium specimens dating back to the 1800s, we have facilitated the rapid identification of this emerging pathogen both for specialists and for nonexperts. This approach not only underscores the importance of historical collections in understanding pathogen evolution but also highlights the application of phylogenetic tools in understanding contemporary agricultural challenges.

The increased prevalence of powdery mildew across global blueberry farms over the last 5 yr has posed new challenges to the industry, notably in yield reductions and the increased need for fungicide applications. The observed absence of powdery mildew on blueberries in the Pacific Northwest (PNW), despite the region's conducive environment for powdery mildew (Bradshaw, 2020), suggests a limited current spread but anticipates a potential future risk. This could also be the case for Australia and central Mexico. It is important to note that in the PNW, agriculture conditions may not be as conducive as in other regions, as blueberries are not grown in tunnels here. This finding indicates the pathogen's possible expansion beyond its current distribution, urging continuous monitoring and research efforts to preemptively address its spread into new regions.

The insights gained from our study pave the way for future research into pathogen spread and invasiveness, and host–pathogen co-evolution. Conducting host range inoculation and virulence trials on the different blueberry formae, as well as comparative genomic analyses of the different formae, will be informative in unraveling the complexities of disease spread. By advancing our knowledge of these plant pathogens and employing phylogenetic approaches, we can enhance our ability to predict, monitor, and control the spread of powdery mildew.

Acknowledgements

We would like to thank the curation team at BPI, CUP, DAOM, FH, GAM, HAL, NCSLG, NR, NYS, and WTU for helping with the herbarium specimens. Additionally, we would like to thank the National Science Foundation, Award no. 2402193, for funding this research. The development of the DeCIFR system and T-BAS was supported by the Novo Nordisk Foundation (https://novonordiskfonden.dk/en/) grant nos. NNF19SA0059360 (INTERACT) and NNF19SA0035476 (CCRP), and from NSF Award nos. 2200038, 2031955, and 2308472.

Competing interests

None declared.

Author contributions

MB designed the manuscript, brought together the team of collaborators, sequenced the specimens, organized the data and wrote the first draft. KI and JCB helped design the manuscript and bring together the team of collectors and acquire introduction data. UB collected specimens and assisted with the taxonomy. SY collected and sequenced specimens from China. IC conducted the population genetics analyses. ML and JC sampled and sequenced the specimens from DAOM. JKM and LQ conducted morphological work. UC and SL helped with specimen and data organization. DHP helped fund and organize the project. EM, BW, WOC, SM, AKL, WA, MEG, RC, ME, DB, TC, JW, JM and ST collected fungal specimens.

ORCID

Michael Bradshaw https://orcid.org/0000-0002-7133-4679

Data availability

The data that support the findings of this study are openly available in GenBank (National Center for Biotechnology Information) and T-Bas (https://guide-tbas.cifr.ncsu.edu/tbas). GenBank numbers are included in Table S1.

References

Abadi S, Azouri D, Mayrose I, Pupko T. 2019. Model selection may not be a mandatory step for phylogeny reconstruction. *Nature Communications* **10**: 1–11.

Álvarez-Escribano I, Sasse C, Bok JW, Na H, Amirebrahimi M, Lipzen A, Schackwitz W, Martin J, Barry K, Gutiérrez G *et al.* 2019. Genome sequencing of evolved aspergilli populations reveals robust genomes, transversions in *A. flavus*, and sexual aberrancy in non-homologous end-joining mutants. *BMC Biology* **17**: 88.

Baranova MA, Logacheva MD, Penin AA, Seplyarskiy VB, Safonova YY, Naumenko SA, Klepikova AV, Gerasimov ES, Bazykin GA, James TY *et al.* 2015. Extraordinary genetic diversity in a wood decay mushroom. *Molecular Biology and Evolution* **32**: 2775–2783.

Barbera P, Kozlov AM, Czech L, Morel B, Darriba D, Flouri T, Stamatakis A. 2019. EPA-NG: massively parallel evolutionary placement of genetic sequences. *Systematic Biology* **68**: 365–369.

Bebber DP, Holmes T, Gurr SJ. 2014. Tracking the global spread of crop pests and pathogens: evidence of significant ecological impacts. *Global Ecology and Biogeography* **23**: 1398–1407.

Besnier F, Glover KA. 2013. PARALLELSTRUCTURE: a R package to distribute parallel runs of the population genetics program STRUCTURE on multi-core computers. *PLoS ONE* **8**: e70651.

Bradshaw M, Braun U, Elliott M, Kruse J, Liu S-Y, Guan G, Tobin P. 2021. Global genetic insights from herbarium specimens reveal invasion dynamics of an introduced fungal plant pathogen. *Fungal Biology* **125**: 585–595.

Bradshaw MJ. 2020. *Epidemiology and biology of powdery mildews and their host plants*. Dissertation, University of Washington, ProQuest Dissertations. [WWW document] URL https://www.proquest.com/docview/2436894555 [accessed 10 June 2024].

Bradshaw M, Braun U, Pfister DH. 2023. Phylogeny and taxonomy of the genera of Erysiphaceae, part 4: *Erysiphe* (the "Uncinula lineage"). *Mycologia* **115**(6): 871–903.

Bradshaw MJ, Boufford D, Braun U, Moparthi S, Jellings K, Maust A, Pandey B, Slack S, Pfister DH. 2024a. An in-depth evaluation of powdery mildew hosts reveals one of the world's most common and widespread groups of fungal plant pathogens. *Plant Disease* **108**: 576–581.

Bradshaw MJ, Braun U, Crouch J, LaGreca S, Pfister DH. 2024b. Phylogeny and taxonomy of the genera of Erysiphaceae, part 6, Erysiphe (the "Microsphaera lineage" part 2). *Mycologia* . Online First. doi: 10.1080/00275514.2024.2386230.

Bradshaw MJ, Braun U, Guan GX, Liu SY, Nokes L, Pfister D. 2022a. Secondary DNA barcodes (*CAM*, *GAPDH*, *GS*, and *RPB2*) to characterize species complexes and strengthen the powdery mildew phylogeny. *Frontiers in Ecology and Evolution* **10**: 918908.

Bradshaw MJ, Quijada L, Tobin P, Braun U, Newlander C, Potterfield P. 2022b. More than just plants: botanical gardens as a source of fungal diversity. *HortScience* **57**: 1289–1293.

Bradshaw MJ, Tobin P. 2020. Sequencing herbarium specimens of a common detrimental plant disease (powdery mildew). *Phytopathology* **110**: 1248–1254.

Braun U, Cook RTA. 2012. *Taxonomic manual of the Erysiphales (powdery mildews)*. Utrecht, the Netherlands: CBS-KNAW Fungal Biodiversity Centre.

Carbone I, White JB, Miadlikowska J, Arnold AE, Magain N, Miller MA, U'Ren JM, Lutzoni F. 2019. T-BAS v.2.1: Tree-Based Alignment Selector toolkit for evolutionary placement of DNA sequences and viewing alignments and specimen metadata on curated and custom trees. *Microbiology Resource Announcements* **8**: e00328-19.

Carbone I, White JB, Miadlikowska J, Arnold AE, Miller MA, Kauff F, U'Ren JM, May G, Lutzoni F. 2017. T-BAS: Tree-Based Alignment Selector toolkit for phylogenetic-based placement, alignment downloads, and metadata visualization; an example with the Pezizomycotina tree of life. *Bioinformatics* **33**: 1160–1168.

Clement M, Posada D, Crandall KA. 2000. TCS: a computer program to estimate gene genealogies. *Molecular Ecology* **9**: 1657–1659.

Cunnington JH, Takamatsu S, Lawrie AC, Pascoe IG. 2003. Molecular identification of anamorphic powdery mildews (Erysiphales). *Australasian Plant Pathology* **32**: 421–428.

Earl DA, vonHoldt BM. 2011. STRUCTURE HARVESTER: a website and program for visualizing STRUCTURE output and implementing the Evanno method. *Conservation Genetics Resources* **4**: 359–361.

Edwards HM, Rhodes J. 2021. Accounting for the biological complexity of pathogenic fungi in phylogenetic dating. *Journal of Fungi* **7**: 661.

Ellingham O, David J, Culham A. 2019. Enhancing identification accuracy for powdery mildews using previously underexploited DNA loci. *Mycologia* **111**: 798–812.

Evanno G, Regnaut S, Goudet J. 2005. Detecting the number of clusters of individuals using the software STRUCTURE: a simulation study. *Molecular Ecology* **14**: 2611–2620.

Falush D, Stephens M, Pritchard JK. 2003. Inference of population structure using multilocus genotype data: linked loci and correlated allele frequencies. *Genetics* **164**: 1567–1587.

Felsenstein J. 1985. Confidence limits on phylogenies: an approach using the bootstrap. *Evolution* **39**: 783–791.

Fu Y-X, Li W-H. 1993. Statistical tests of neutrality of mutations. *Genetics* **133**: 693–709.

Fuller KB, Alston JM, Sambucci OS. 2014. Evaluating the economic value of powdery mildew resistance in California grape production. *Journal of Agricultural Economics* **67**: 132–146.

Futuyma DJ, Moreno G. 1988. The evolution of ecological specialization. *Annual Review of Ecology and Systematics* **19**: 207–233.

Gernhard T. 2008. The conditioned reconstructed process. *Journal of Theoretical Biology* **253**: 769–778.

Hey J, Chung Y, Sethuraman A, Lachance J, Tishkoff S, Sousa VC, Wang Y. 2018. Phylogeny estimation by integration over isolation with migration models. *Molecular Biology and Evolution* **35**: 2805–2818.

Hey J, Wakeley J. 1997. A coalescent estimator of the population recombination rate. *Genetics* **145**: 833–846.

Hirata T, Takamatsu S. 1996. Nucleotide sequence diversity of rDNA internal transcribed spacers extracted from conidia and cleistothecia of several powdery mildew fungi. *Mycoscience* **37**: 283–288.

Homma Y. 1937. Erysiphaceae of Japan. *Journal of the Faculty of Agriculture of the Hokkaido Imperial University* **38**: 208–209.

Huson DH. 1998. SPLITSTREE: analyzing and visualizing evolutionary data. *Bioinformatics* **14**: 68–73.

Jailloux F, Thind T, Clerjeau M. 1998. Release, germination, and pathogenicity of ascospores of *Uncinula necator* under controlled conditions. *Canadian Journal of Botany* **76**: 777–781.

Jarvis WR, Gubler WD, Grove GG. 2002. Epidemiology of powdery mildews in agricultural pathosystems. In: Bélanger R, Dik AJ, Bushnell WR, eds. *The powdery mildews: a comprehensive treatise*. St Paul, MN, USA: APS Press, 169–199.

Johnson JW, Baenziger PS, Yamazaki WT, Smith RT. 1979. Impact of powdery mildew on the yield and quality of isogenic lines of 'Chancellor' wheat. *Crop Science* **19**: 349–352.

Kiss L, Vaghefi N, Bransgrove K, Dearnaley JDW, Takamatsu S, Tan YP, Marston C, Liu S-Y, Jin D-N, Adorada DL *et al.* 2020. Australia: a continent without native powdery mildews? The first comprehensive catalogue indicates recent introductions and multiple host range expansion events, and leads to the re-discovery of Salmonomyces as a new lineage of the Erysiphales. *Frontiers in Microbiology* **11**: 1571.

Kusch S, Qian J, Loos A, Kümmel F, Spanu PD, Panstruga R. 2024. Long-term and rapid evolution in powdery mildew fungi. *Molecular Ecology* **32**: 1263–1279.

Miller MA, Schwartz T, Pickett BE, He S, Klem EB, Scheuermann RH, Passarotti M, Kaufman S, O'Leary MA. 2015. A RESTful API for access to phylogenetic tools via the CIPRES science gateway. *Evolutionary Bioinformatics Online* **11**: 43–48.

Mori Y, Sato Y, Takamatsu S. 2000. Evolutionary analysis of the powdery mildew fungi using nucleotide sequences of the nuclear ribosomal DNA. *Mycologia* **92**: 74–93.

Pritchard JK, Stephens M, Donnelly P. 2000. Inference of population structure using multilocus genotype data. *Genetics* **155**: 945–959.

Rambaut A. 2009. *FIGTREE v.1.3.1*. [WWW document] URL http://tree.bio.ed.ac.uk/software/figtree

Salmon E. 1900. A monograph of the Erysiphaceae. *"Memoirs" of the Torrey Botanical Club* **9**: 9.

Silvestro D, Michalak I. 2012. RAXMLGUI: a graphical front-end for RAxML. *Organisms Diversity & Evolution* **12**: 335–337.

Sotiropoulos AG, Arango-Isaza E, Ban T, Barbieri C, Bourras S, Cowger C, Czembor PC, Ben-David R, Dinoor A, Ellwood SR *et al.* 2022. Global genomic

analyses of wheat powdery mildew reveal association of pathogen spread with historical human migration and trade. *Nature Communications* **13**: 4315.

Suchard MA, Lemey P, Baele G, Ayres DL, Drummond AJ, Rambaut A. 2018. Bayesian phylogenetic and phylodynamic data integration using BEAST 1.10. *Virus Evolution* **4**: vey016.

Tajima F. 1989. Statistical method for testing the neutral mutation hypothesis by DNA polymorphism. *Genetics* **123**: 585–595.

Tamura K, Stecher G, Kumar S. 2021. MEGA11: molecular evolutionary genetics analysis v.11. *Molecular Biology and Evolution* **38**: 3022–3027.

Tymon LS, Bradshaw M, Götz M, Braun U, Peever TL, Edmonds RL. 2022. Phylogeny and taxonomy of *Erysiphe* spp. on Rhododendron with a special emphasis on North American species. *Mycologia* **114**: 887–899.

Vaghefi N, Kusch S, Németh MZ, Seress D, Braun U, Takamatsu S, Panstruga R, Kiss L. 2022. Beyond nuclear ribosomal DNA sequences: evolution, taxonomy, and closest known saprobic relatives of powdery mildew fungi (Erysiphaceae) inferred from their first comprehensive genome-scale phylogenetic analyses. *Frontiers in Microbiology* **13**: 903024.

Walsh PS, Metzger DA, Higuchi R. 1991. Chelex 100 as a medium for simple extraction of DNA for PCR–based typing from forensic material. *BioTechniques* **10**: 506–513.

Woerner AE, Cox MP, Hammer MF. 2007. Recombination-filtered genomic datasets by information maximization. *Bioinformatics* **23**: 1851–1853.

Yi X, Latch EK. 2021. Nonrandom missing data can bias Principal Component Analysis inference of population genetic structure. *Molecular Ecology Resources* **22**: 602–611.

Zang J. 2022. *IBO reports on status of global blueberry industry.* Produce report. [WWW document] URL https://www.producereport.com/article/ibo-reports-status-global-blueberry-industry [accessed 10 June 2024].

Zhang C, Rabiee M, Sayyari E, Mirarab S. 2018. ASTRAL-III: polynomial time species tree reconstruction from partially resolved gene trees. *BMC Bioinformatics* **19**: 153.

Supporting Information

Additional Supporting Information may be found online in the Supporting Information section at the end of the article.

Fig. S1 Maximum likelihood and ASTRAL phylogenies inferred from seven loci (*CAM*, *GAPDH*, *GS*, ITS, LSU, *RPB2*, *TUB*).

Fig. S2 Statistical parsimony haplotype network showing the geographical distribution of haplotypes.

Fig. S3 Population structure, haplotype, geographic, and forma distribution. Colorized rings around the tree are used to show different strain attributes.

Table S1 Specimens evaluated in the present study.

Table S2 Farms where powdery mildew was collected from and associated data.

Table S3 Species, clade, strain, and multilocus haplotype distribution.

Table S4 Population parameter estimates in six *Erysiphe* forma.

Please note: Wiley is not responsible for the content or functionality of any Supporting Information supplied by the authors. Any queries (other than missing material) should be directed to the *New Phytologist* Central Office.

Disclaimer: The New Phytologist Foundation remains neutral with regard to jurisdictional claims in maps and in any institutional affiliations.